Development of an artefact to detect unfused powder in additive manufactured components using X-ray CT

Ahmed Tawfik[1], Paul Bills[1], Liam Blunt[1], Radu Racasan[1]
[1]EPSRC Future Advanced Metrology Hub, School of Computing and Engineering, University of Huddersfield, Huddersfield, United Kingdom, e-mail: Ahmed.Tawfik@hud.ac.uk

Abstract
Assessing functional performance is the most important stage of any component verification. Mechanical properties can be evaluated by means of destructive testing which can be both expensive and lengthy in addition to loss of the original component under test. It is therefore advantageous where possible to utilise non-destructive techniques that can achieve the same or similar outcomes through collection of three-dimensional data that can then be used in simulation to determine functionality. Such non-destructive methods with 3D location ability are essentially density- and porosity-based testing methods. Additive manufacturing allows the creation of complex geometrical features that are often defined based on function. Optimisation of AM component geometry based on functionality allows for the specification of components that have features that cannot be mapped efficiently to current GPS standards ISO 14638. In addition, the integrity of complex optimised AM structures that may lie on a critical stress or heat path must be assessed and any elements of unfused powder for example, must be detected. This seeks to investigate the ability of X-ray computer tomography to detect and characterised small scale empty and powder filled defects which may occur in AM manufactured parts. To achieve this, aim a Ti6AL4V artefact built using an Arcam Q10 electron beam-melting machine (EBM). Defects of between 50 and 1400 microns in diameter were machined into the surface of the artefact using a precision CNC machine equipped with micro-drills. Once this was achieved, the defects were characterised using focus variation microscope. Virgin Ti6AL4V powder was added to fill 50% of the defects and then the artefact was measured using a Nikon XTH225 industrial CT. This was used to analyse the relative size and volume of the defects and assess the capability of the inspection process to both assess the size of pores and to detect the powder-filled defects. To reduce the number of process variables, all the measurement process parameters, such as filament current, acceleration voltage and X-ray filtering material and thickness, were kept constant between the scans with hollow and powder filled defects. The acquired data processing, surface determination process and defect analysis was carried out using VgStudio Max (Volume Graphics, Germany). The focus of the study is on providing best practice regarding the selection of inspection parameters and identifying the capability of the process to detect unfused powder.

Keywords: Unfused powder, Defects analysis, Additive Manufacturing, Computer tomography

1. Introduction

There are various non-destructive test methods to detect internal defects/pores in AM manufactured parts, for example Archimedes, metallography and ultrasonic techniques. These methods however do not provide accurate information about pore size, shape or distribution. A recent study has shown that the shape and location of the pore must be considered to avoid premature failure of AM parts under stress. (Lambert, Chambers, Sinclair & Spearing, 2012).

X-ray computer tomography (CT) is a non-destructive test method that has the capability to detect porosity whilst analysing the component volume providing position, location distribution and volume of any pores/defects. In this method the component is placed on a rotating stage and an X-ray beam is projected through the specimen before the transmitted X-ray are collected at a detector. Back projection algorithms filter the obtained data and after reconstruction a 3D model is then created. There are several available methods that can be used to analyse the data, a common method being converting the data file to an STL prior to analysis using Matlab. Other methods require the use of proprietary software (e.g. Volume Graphics VG Studio Max) to threshold and to differentiate between the grey values of the object material and the background. This often involves the use of ISO 50 surface determination; then advanced segmentation algorithms can be applied to carry out the defect analysis. (Yagüe-Fabra et al., 2013).

The pores/defects in additively manufactured components are different to those typically seen in cast components. The pores in cast components are usually hollow and filled with gas, in the AM component the pore could be either hollow, filled with unfused powder or filled with partially fused powder. The unfused powder grains can be of the order of 45µm diameter (AP&C, 2017) when considering EBM manufactured components and 15µm diameter for selective laser melted (SLM) components (Slm-solutions.com, 2017). Functionally powder filled pores are equally deleterious to part properties and as such it is critical they are located and assessed.

Nikishkov et al. investigated CT measurements for porosity using a unidirectional Carbon/Epoxy tape composite artefact designed with microscopic holes accessible from the surface. The artefact was scanned with a CT and the results were compared to the measurements obtained by microscopy (Nikishkov, Airoldi & Makeev, 2013). The artefact did not contain internal pores/defects due to the holes being accessible from the surface.

Jansson et al. designed an artefact containing micro internal pores/defects and manufactured it using the SLM additive manufacturing process. The defects were measured solely using a CT machine therefore the author relied extensively on the ability and accuracy of the manufacturing process (A. Jansson, 2015). The results of the study were not confirmed by any alternative method or physical sectioning.

Hermanek et al. developed an aluminium artefact shown in figure 1 to determine the accuracy of CT porosity measurements when scanning using different parameters. This artefact featured micro-milled hemispherical defects with a diameter ranging from 120µm to 500µm. (Hermanek & Carmignato, 2016). This experiment was limited to hollow defect/pores that are filled with air. When considering additively manufactured components especially powder bed applications the defects/pores can contain unfused or semi-fused powder.

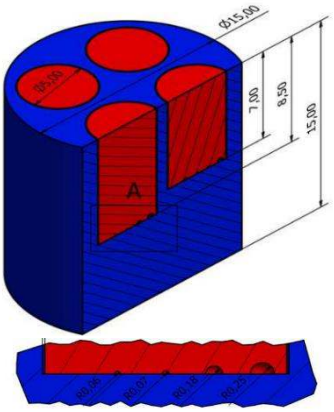

Figure 1 Aluminium artefact with micro drilled hemispherical features (Hermanek & Carmignato, 2016)

2. Study Rationale

When conducting an earlier NDT study the author scanned a 16 x 16 mm square titanium bar manufactured using an EBM machine shown in figure 2. The component was scanned with a voxel size of 38 µm. The subsequent defect analysis based on XCT results did not detect any unfused powder within the component. To confirm the XCT results the component was sectioned. It was evident when sectioning the component that some defects were not detected by the XCT and when sectioning the component unfused powder was liberated and evidence of semi-fused powder was also found under examination with a microscope as shown in figure 3. Detecting such filled pores/defects is challenging and the process is governed by the size of the pore and the size of the component. The above reasons have driven the need to design an artefact with calibrated internal defects that can be filled with powder and are accessible to be measured with conventional non-contact metrology instruments. The defects can then be scanned using a CT to determine size, volume and position. The difference in volume between the hollow and powder filled defects can then be evaluated. Figure 4 shows an SEM image of virgin Ti6aL4V ELI powder that was used for this study. The particles are uniform and spherical in shape with sizes ranging from 45µm to 100 µm. The spherical shape and the size variation poses a big challenge for detection with XCT, due to the smaller powder particles filling the gaps between the bigger ones.

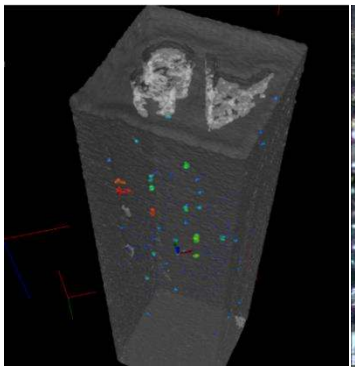

Figure 2 Defects analysis for titanium AM part

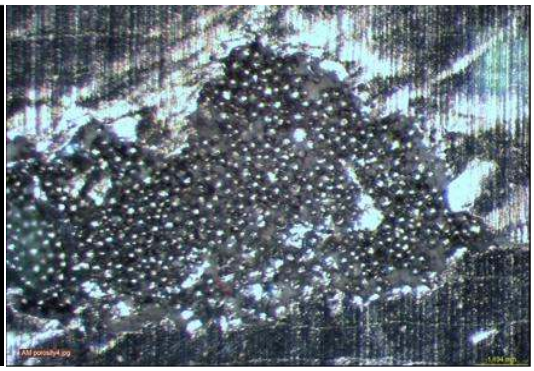

Figure 3 Semi fused powder

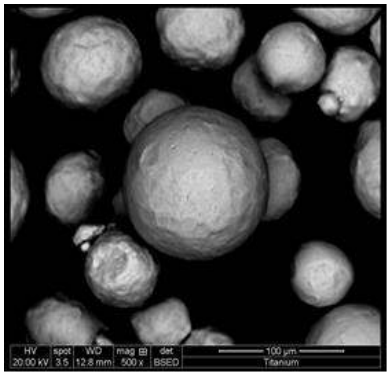

Figure 4 SEM image of virgin Ti6aL4V powder

3. Artefact development

This study investigates the ability of XCT methods to differentiate between hollow defects and powder filled defects. Powder filled defects are of particular interest and concern in the burgeoning area of additive manufacturing. In this experiment a Nikon XTH225 industrial XCT was used to characterise a Ti6AL4V artefact built using an Arcam Q10 electron beam-melting machine (EBM). Prior to measurement 50, 100, 500 and 1400µm holes were drilled onto the polished surface of the artefact using a CNC machine equipped with micro drills and end mills as shown in figure 5, the holes are in this case selected to be representative of typical defects. The specific dimensions for the defects were selected based on actual pores identified earlier within the AM produced bar described above. The 1.4mm and 0.5mm diameter holes were selected to be filled with powder whilst the 50 and 100µm diameter holes were left as voids.

In the case of the EBM AM machine used in this study the powder deposition layer thickness is approximately 40µm (Dsiac.org, 2017) therefore the 50µm defect will reproduce that which could occur due to disruption of a single layer. The 100µm defect will similarly replicate a two layer disruption. The surface was machined using a diamond cut finish whilst the mating part with the same diameter was designed to enclose the drilled holes thus creating internal defects/pores. The principle of ringing the two surfaces together is similar to that employed for slip gauges. Consequently, the XCT will was not able to detect the gap and thus they can be considered as a single component with internal defects. Prior to ringing the parts the defects were characterised using a focus variation microscope (Alicona G4) to determine the reference values for the diameter and defect depth. Note the Alicona was calibrated per the manufacturers recommendations (Alicona – That's metrology, 2017) . The artefact was then scanned with XCT to determine any differences between hollow and powder filled defects. The scanning parameters shown in table 1 were kept constant throughout the experiment.

Table 1. Settings used for CT measurements

Filter	0.5mm Cu
Exposure	4000 ms
Filament current	58 uA
Acceleration voltage	157 Kv
Voxel size	7.4 µm
Gain	12

To ensure that the artefact is fit for purpose and can be used as a reference object to investigate unfused powder and hollow pore detection, the following requirements must be satisfied:

1- The parts should be made using a additive manufacturing technique
2- The material used should be relevant for industrial applications
3- The artefact dimensions and defect dimensions should replicate a scenario that is relevant to industrial use.

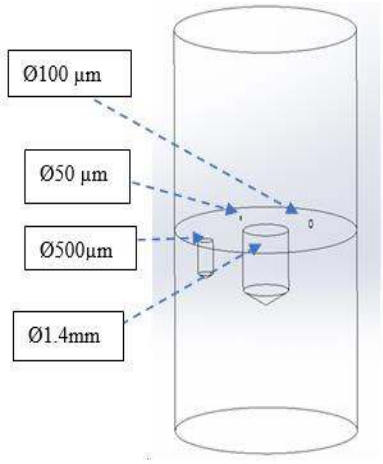

Figure 5 Artefact 3D model

Figure 6-a shows the actual surface for the lower half of the artefact containing the manufactured 1.4mm and 0.5mm /defects filled with titanium powder whilst the 50µm and the 100µm holes remain unfilled shown in figure 5.
The drilled holes were measured using an AliconaG4 focus variation microscope and diameter and volume values were then calculated from the data by assuming that each hole consists of a combined cylinder and cone. The volume and diameter of each hole was compared to the design data in figure 14 and 15.
The Alicona and CT results are given in Table 2 showing the defect size and volume information the as calculated based on equations below

Table 2 Designed Defects values and calculated volume

Defect	1	2	3	4
Diameter	1.4mm	500µm	100µm	50µm
Depth	2mm	1mm	210µm	100µm
Volume	2.870mm^3	0.193mm^3	0.001mm^3	0.000 mm^3

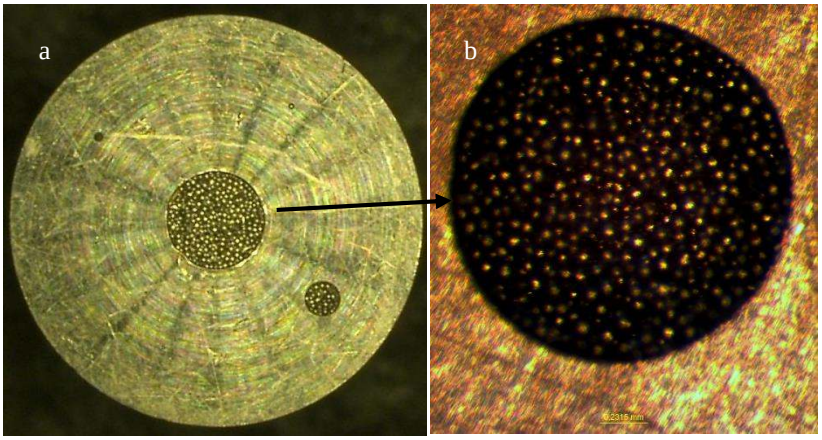

Figure 6 a) Artefact lower half with holes filled with powder, b)1.4mm defect filled with powder

4. Results

There are three main measurements performed in this experiment. Firstly the defects were measured using the Alicona, secondly the defects were scanned using XCT without powder and thirdly the defects were scanned once powder filled. The depth, diameter and volume of each defect will be compared between the AliconaG4 and XCT.

4.1 Alicona defects measurement

The AliconaG4 instrument uses a non-contact focus variation method to determine the defects diameter and depth. The focus variation method works by capturing images with different focus depths, changes in focus occur by moving the optics or the work piece in relation to each other. The focus over each plane is analysed for each position on the specimen, then the plane with best focus is selected for each position on the part. The focus variation method has excellent slope detection ability, can be used to measure uneven surfaces, detect colour information but cannot be used with reflective surfaces ex: polished metals or glass (Fundamental Principles of Engineering Nanometrology, 2017).

Table 3 Alicona Defects dimensions and calculated volume

Defect	1	2	3	4
Diameter	1.434mm	526µm	142µm	86µm
Depth	2.157mm	1.090mm	280µm	12µm
Volume	3.000mm^3	0.215mm^3	0.004mm^3	0.000 mm^3

The defect diameters were measured by using a three point best fit circle. The depth was measured by selecting two points on the upper surface and creating a horizontal line and a point on the lowest point in the drilled hole.
In figure 7 and 8 defect 1 is shown as having a radius of 717.30µm and a depth of 2.158mm. Table 3 shows the complete list of values for diameter, depth and calculated volume for all defects of the artefact as measured using the Alicona. The depth for defect 4 was not accurately measured as the obtained result was 12µm, it was expected to be 100µm. This result is not correlating with the CNC machine depth and subsequent CT inspection. The likely cause for this is the inability of the instrument to image the bottom of the hole using the selected magnification.

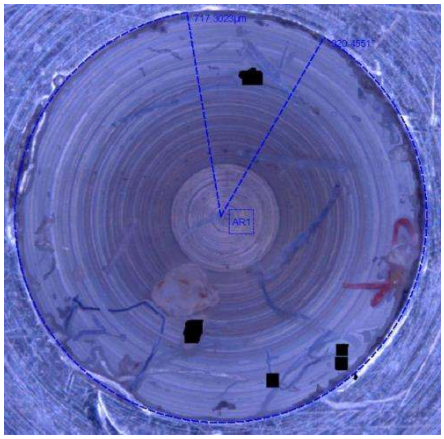

Figure 7 Alicona value for defect 1 radius

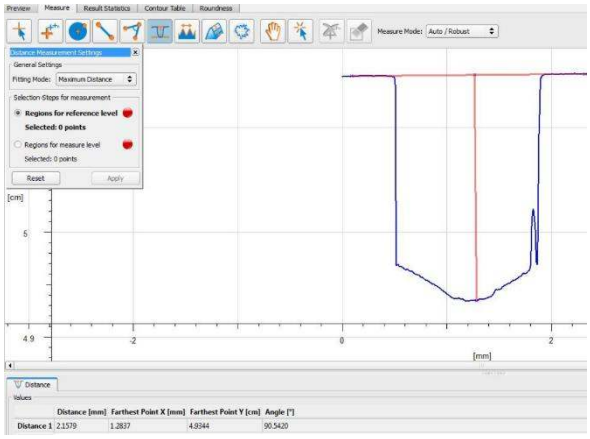

Figure 8 Alicona value for defect 1 depth

4.2 XCT hollow defects results

In this section the results obtained by XCT for the hollow defects are presented. The artefact was scanned at a voxel size of 7.4 µm using a Nikon 225 XTH. The data was analysed using Volume Graphics VGStudio Max 3.0.3. The diameter was determined by using best fit geometry measurements based on the surface determination. Three points were selected on the diameter creating to generate a circle. The depth was evaluated using the distance measurement by selecting the highest and lowest point in the defect.
This method for measuring the defect dimensions is influenced by the accuracy with which surface determination is performed. The overall scan quality and the accuracy of surface determination can be assessed by measuring the dimension of designed internal defects and comparing this with microscopy measurements.

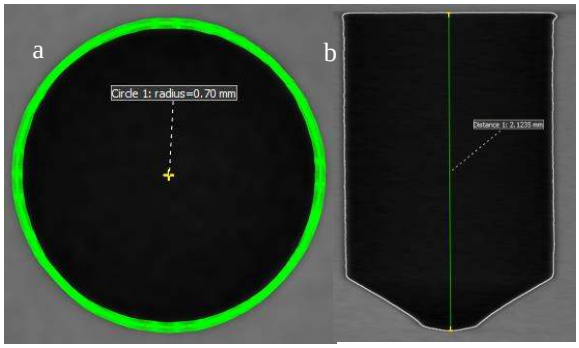

Figure 9 a) XCT image for defect 1 with measured radius, b) XCT value for defect 1 depth

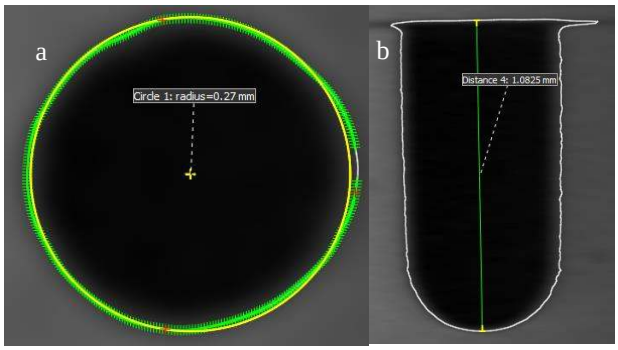

Figure 10 a) Figure 7 XCT image for defect 2 with measured radius, b) XCT value for defect 2 depth

Figures 10-a and 10-b show the diameter and depth values for defect 1. The CT values are 1.434mm and 2.12mm respectively, Figures 11-a and 11-b show the diameter and depth for defect 2, CT values are 0.540mm and 0.07mm respectively. It was noted that the defect upper diameter is not perfectly circular. This was also confirmed when performing the Alicona measurements.

Table 4 XCT values for diameter depth and volume

Defect	1	2	3	4
Diameter	1.426mm	533µm	149µm	82µm
Depth	2.120mm	1.082mm	306µm	71µm
Volume	3.046mm^3	0.220mm^3	0.0052mm^3	0.0008 mm^3
Volume (Alicona)	3.000mm^3	0.215mm^3	0.004mm^3	0.000 mm^3

The defects volume obtained from the XCT show a good correlation with Alicona volume results apart from defect 4. As stated previously the depth measured using the Alicona for defect 4 depth is not accurate, therefore the volume difference between the two instruments for defect 4 will be considered wrong.

4.3 XCT defects filled with powder results

To test the capability of the XCT system in detecting unfused powder defect 1 and 2 were filled with the same powder that was used to manufacture the artefact. The measurements used the same settings and voxel size as in the first scan. The porosity analysis was carried out in VGStudio Max to detect the volume of each defect. The volume of defect 1 filled with powder was 2.319mm^3 and the defect 2 volume was 0.166 mm^3. Figure 14 shows a 3D image of the artefact with defect 1 and 2 filled with powder. The model reconstruction, surface determination and porosity analysis was carried out without any noise filtration. The main reason for not using noise filtration is to avoid mixing micro voids with “noise particles”.

Figure 15 and 16 shows 2D images for defect 1 and 2. The air gaps between the powder particles are not uniform owing to the difference in the diameter and shape of the powder particles but it is evident using the correct XCT settings that it is possible to identify the existence of powder and the overall shape of the defect as well as the size of some of the cavities between particles.

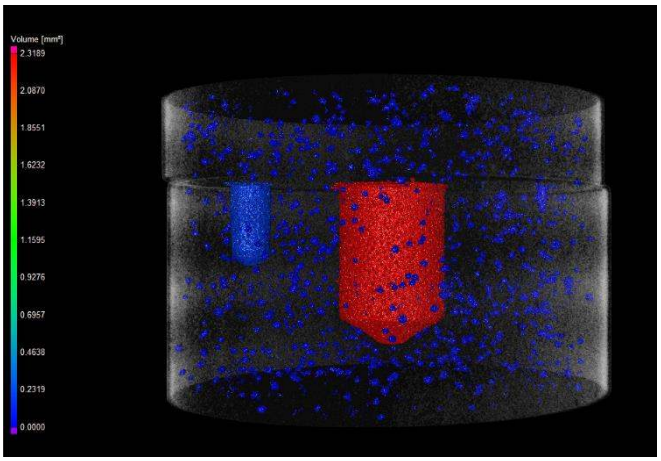

Figure 11 XCT 3D for the powder filled defects

Figure 12 2D image of defect 1

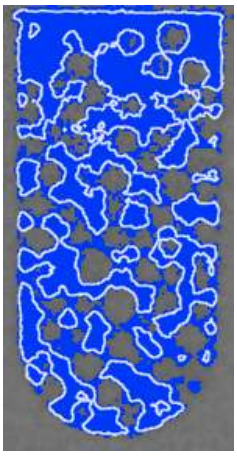

Figure 13 2D image of defect 2

5. Discussion

The results obtained in this study confirm the ability of XCT measurements to quantify accurately internal defect dimensions. A comparison between defects diameters is shown in figure 14 based on the results from Alicona and XCT. The difference in diameter between the designed dimensions and Alicona results for defect 1 and 2 are within 2%, for defect 3 and 4 are 42% and 58% respectively. This big difference in the diameter of the smaller defects could be due to the slight warpage in the part combined with operator error in clamping the part in the CNC machine.

When comparing the Alicona and XCT diameter results the difference was noticeably small. For defect1 the XCT diameter result is 0.55% less than the Alicona result. For defect 2 the XCT diameter is 1.32% larger compared to the Alicona result. conversely for defect 3 there is a 4.7% difference and a 4.6% for defect 4.

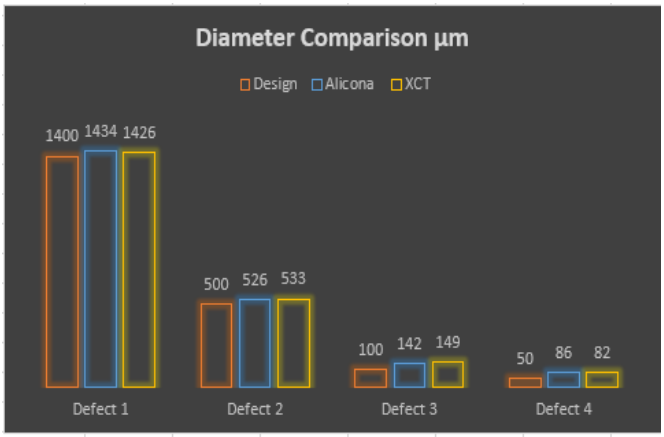

Figure 14 Defects Diameter comparison µm

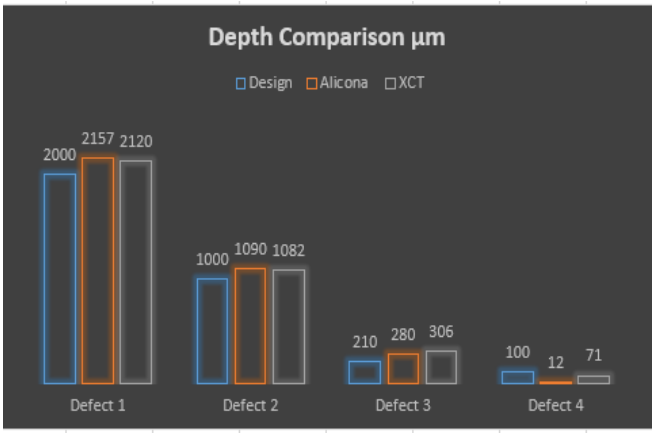

Figure 15 Defects Depth comparison µm

Figure 15 shows a comparison of the defects' depth measurement results. For defect 1 the XCT result is 1.7% less than Alicona result while for defect 2 the XCT result is 0.7% less than the Alicona. The results for defect 3 show 8.5% difference. For defect 4 the Alicona depth measurement result should be ignored due to the inability of the instrument to correctly image the bottom of the defect. .

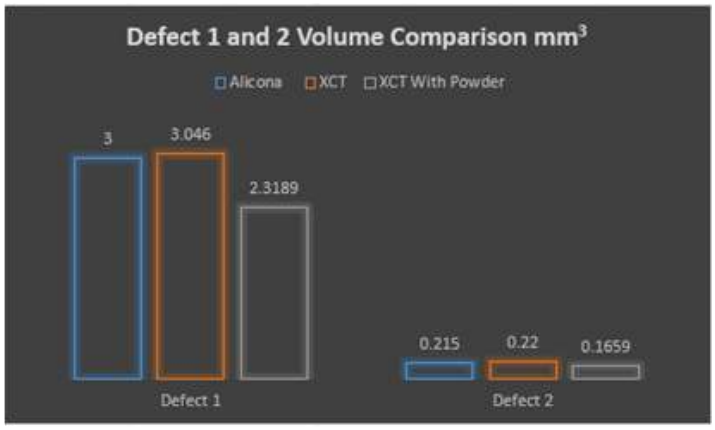

Figure 16 Defect 1 and 2 volume comparison

A comparison between the volume calculated from the Alicona and those obtained from XCT scans with no powder and XCT scan of defects filled with powder is shown in figure 16. The volume from Alicona was calculated assuming the defect shape is formed from a cylinder and a cone, both volumes were added together giving the overall volume of each defect. This method of calculating the volume has a small error due to the radius at the bottom of the cone. The volume results for XCT are obtained from the porosity analysis module in VGStudio Max3.03 which is influenced by the surface determination.

The calculated value of the defect volume (defect 1) as determined by the Alicona was found to be 0.046mm^3 less than the value returned from the XCT analysis of the defect without powder. It is noticeable that there is a 0.73mm^3 (24.3%) decrease in volume between the value returned by the XCT analysis when imaging defects without powder and with powder.

In the case of defect 2 the Alicona calculated volume is 0.005mm^3 less than XCT (2% difference). However, there is a 0.0541mm^3 decrease (25.1%) in calculated volume between XCT results of the defect filled with powder as compared with the void volume.
This small difference implies that using the porosity module we are able to identify the existence of the powder but have failed to quantify it entirely. This could be due to the size of cavities between the powder particles where small particles are filling the cavities between the bigger particles. This error in quantifying will be investigated further.

6.0 Conclusions

The results of this study suggest that detection of small size pores/defects is essential for quantifying larger industrially relevant defects that contain the presence of powder. This experiment proved that the XCT is capable of identifying a difference between hollow/fully voided defects and those which contain unfused powder.

The developed artefact enables the user to create relevant sized defects and evaluate the capability of the defect analysis inspection process. Future work will explore scanning the same artefact using a higher voxel size and comparing the results of the dimensions and volume. Developing a bigger diameter artefact with smaller defects, this will permit the investigation of smaller defects and assessing the ability of XCT in detecting sub 40µm pores.

The mechanical properties of solid material, semi fused and un-fused powder have been shown to be completely different. As such, it is well understood that a solid component will always out perform any component with internal defects. The size and quantity of acceptable internal defects is solely depending on the design intent, the most important and challenging operation in any component validation is correctly accessing it, ensuring that it meets its design intent. It remains to be determined as to the criticality of small volume pores and indeed in non-safety, non-critical and partially optimised components where small volume pores may be largely insignificant to the performance of the component. However, experience suggests that in components that may undergo cyclic heat or mechanical stress this may well be a source of early fatigue failure and as such repeatable and reliable XCT analysis methods are essential for the development of complex functional and optimised AM structures, given the ubiquity and inherent potential of the technology.

Whilst scanning at high magnification undoubtedly improves the accuracy of the obtained results there are significant practical limitations in doing this. In an industrial environment, it is not practical to use scanning strategies that have high acquisition times or are limited to small sample volumes.

References

[1] 14638:2015, I. (2017). ISO 14638:2015 - Geometrical product specifications (GPS) -- Matrix model. [online] Iso.org. Available at: https://www.iso.org/standard/57054.html [Accessed 14 Dec. 2017].

[2] Hermanek, P., & Carmignato, S. (2016). Reference object for evaluating the accuracy of porosity measurements by X-ray computed tomography. Case Studies In Nondestructive Testing And Evaluation, 6, 122-127. http://dx.doi.org/10.1016/j.csndt.2016.05.003

[3] Ontiveros, S., Yagüe-Fabra, J., Jiménez, R., Tosello, G., Gasparin, S., & Pierobon, A. et al. (2012). Dimensional measurement of micro-moulded parts by computed tomography. Measurement Science And Technology, 23(12), 125401. http://dx.doi.org/10.1088/0957-0233/23/12/125401

[4] Yagüe-Fabra, J., Ontiveros, S., Jiménez, R., Chitchian, S., Tosello, G., & Carmignato, S. (2013). A 3D edge detection technique for surface extraction in computed tomography for dimensional metrology applications. CIRP Annals - Manufacturing Technology, 62(1), 531-534. http://dx.doi.org/10.1016/j.cirp.2013.03.016.

[5] Nikishkov, Y., Airoldi, L., & Makeev, A. (2013). Measurement of voids in composites by X-ray Computed Tomography. Composites Science And Technology, 89, 89-97. http://dx.doi.org/10.1016/j.compscitech.2013.09.019

[6] A. Jansson, A.R. Zekavat, L. Pejryd (2015). Measurement of internal features in additive manufactured components by the use of computed tomography Digital Industrial Radiology and Computed Tomography (DIR 2015) Ghent (2015)

[7] AP&C. (2017). Powders designed for Additive Manufacturing - AP&C. [online] Available at: http://advancedpowders.com/our-plasma-atomized-powders/spherical-powders-designed-for-additive-manufacturing/ [Accessed 13 Dec. 2017].

[8] Slm-solutions.com. (2017). Selective Laser Melting Machine SLM 500 | SLM Solutions. [online] Available at: https://slm-solutions.com/products/machines/selective-laser-melting-machine-slm-500 [Accessed 13 Dec. 2017].

[9] Alicona – That's metrology. (2017). InfiniteFocus. [online] Available at: http://www.alicona.com/products/infinitefocus/ [Accessed 20 Dec. 2017].

[10] Fundamental Principles of Engineering Nanometrology. (2017). Google Books. Retrieved 20 June 2017, from https://books.google.co.uk/books?hl=en&lr=&id=jOrEAgAAQBAJ&oi=fnd&pg=PP1&dq=Leach,+R.K.+(2009).+Fundamental+Principles+of+Engineering+Nanometrology,+William+Andrew,+Oxford.&ots=BM45vXo7H5&sig=RgaMrCoznSvloFjBotGjNdCjxXw#v=onepage&q&f=false

[11] Dsiac.org. (2017). Nondestructive Inspection of Additive Manufactured Parts in the Aerospace Industry | DSIAC. [online] Available at: https://www.dsiac.org/resources/journals/dsiac/summer-2016-volume-3-number-3/nondestructive-inspection-additive [Accessed 15 Dec. 2017.

[12] Lambert, J., Chambers, A., Sinclair, I., & Spearing, S. (2012). 3D damage characterisation and the role of voids in the fatigue of wind turbine blade materials. Composites Science And Technology, 72(2), 337-343. http://dx.doi.org/10.1016/j.compscitech.2011.11.023